Enhanced activity and stability of Co_3O_4-decorated nitrogen-doped carbon hollow sphere catalysts for microbial fuel cells

Liang Tan[a], Yi-Dong Yang[b], Nan Li [a,*], Shuang Chen[a], Zhao-Qing Liu[a,*]

[a]School of Chemistry and Chemical Engineering/Guangzhou Key Laboratory for Environmentally Functional Materials and Technology, Guangzhou University, Guangzhou 510006, P. R. China

[b]Affiliated High School of South China Normal University, Guangzhou University, Guangzhou 510006, P. R. China

Fax: 86-20-39366908; Tel: 86-20-39366908;

E-mail:nanli@gzhu.edu.cn (N. Li); lzqgzu@gzhu.edu.cn (Z. Q. Liu)

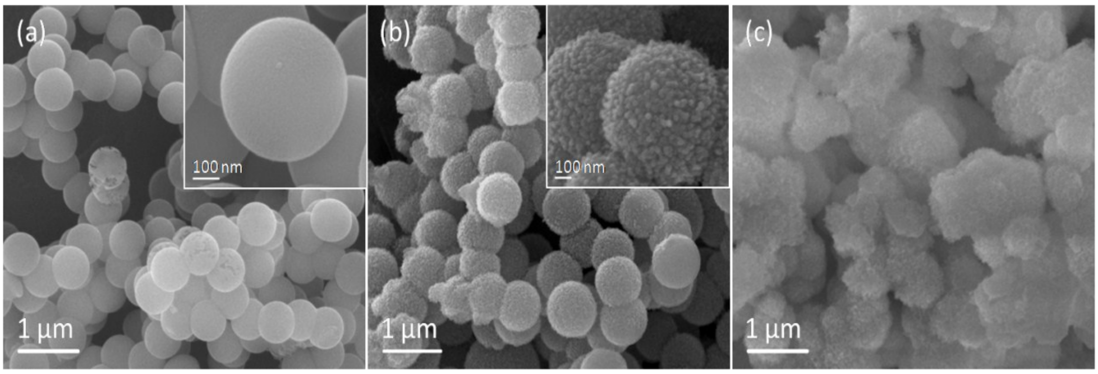

Fig. S1. (a) SEM images of nitrogen-doped carbon spheres; (b) SEM image of CN-Co_3O_4; (c) SEM image of Co_3O_4.

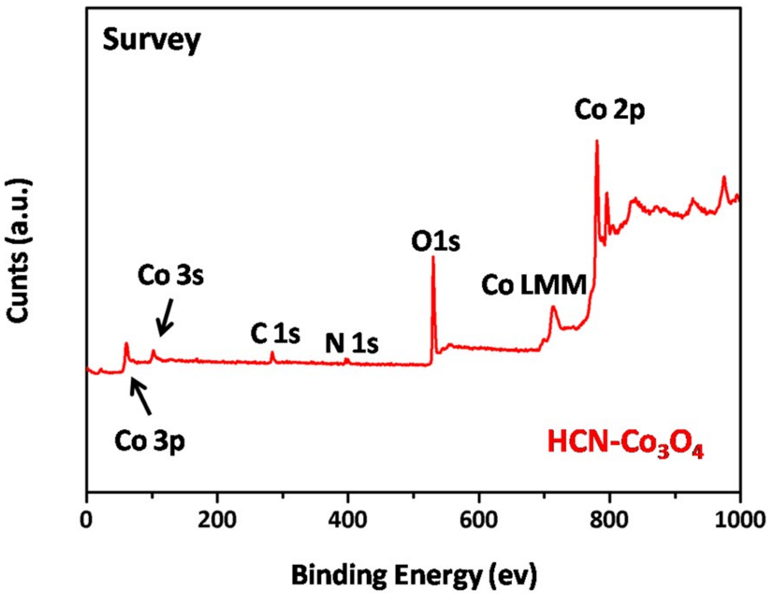

Fig. S2. XPS survey spectra of HCN-Co_3O_4.

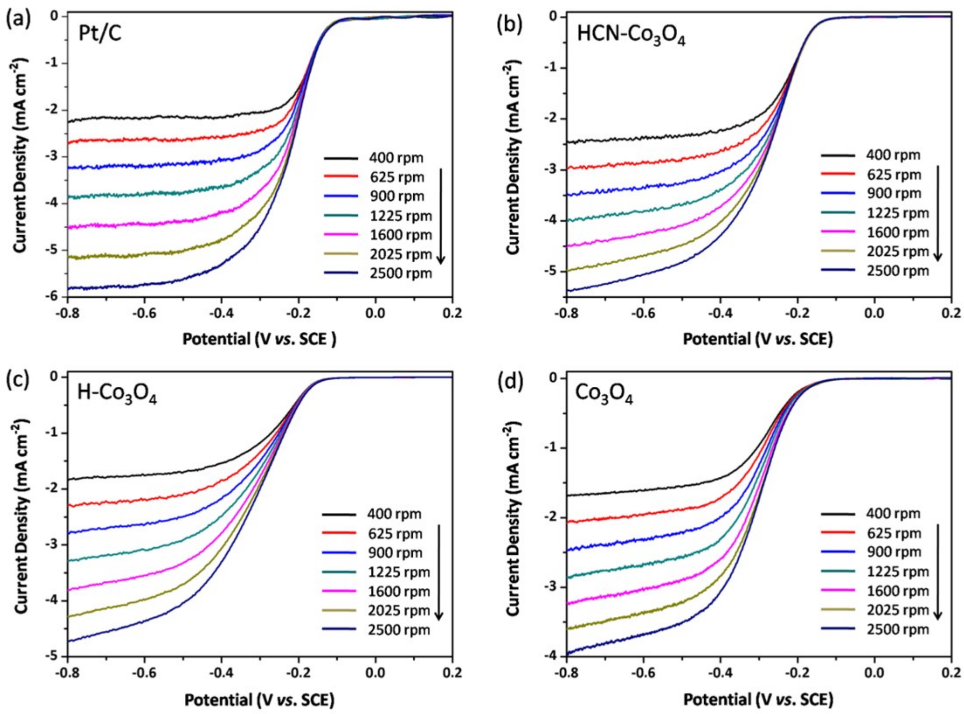

Fig. S3. LSV curves under the different rotational speed from 400 to 2500 rpm at the 0.1 M KOH solution for different samples.

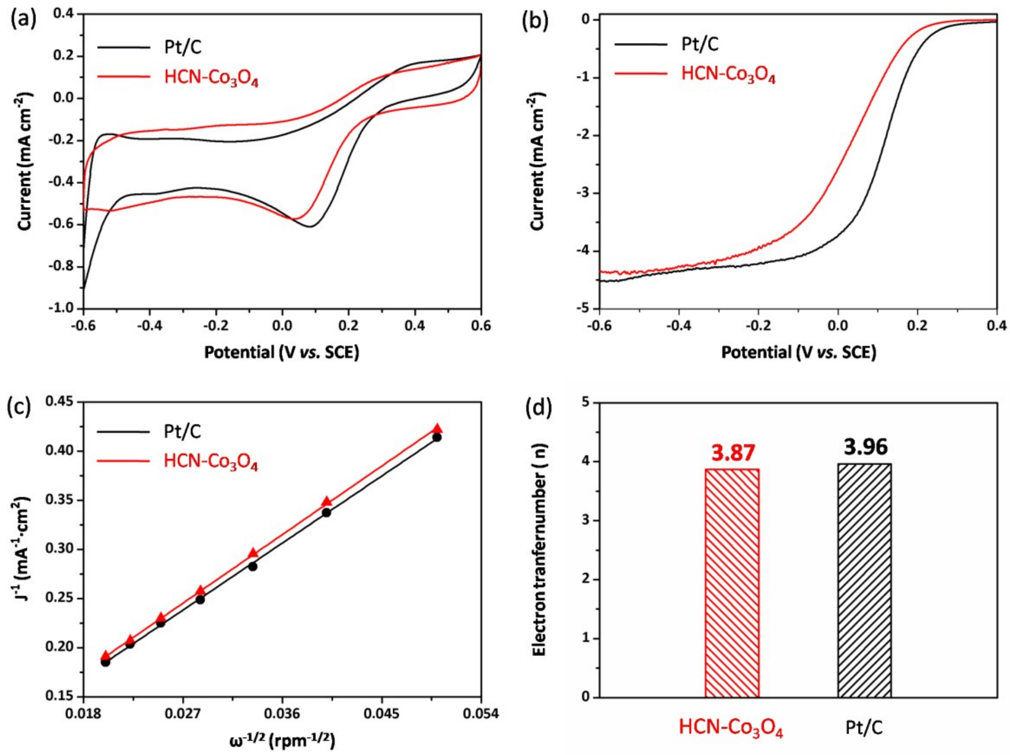

Fig. S4. (a) CV and (b) LSV curves of Pt/C and HCN-Co_3O_4 obtained at 0.05 M PBS; (c) K-L curves and (d) electron transfer numbers of Pt/C and HCN-Co_3O_4.

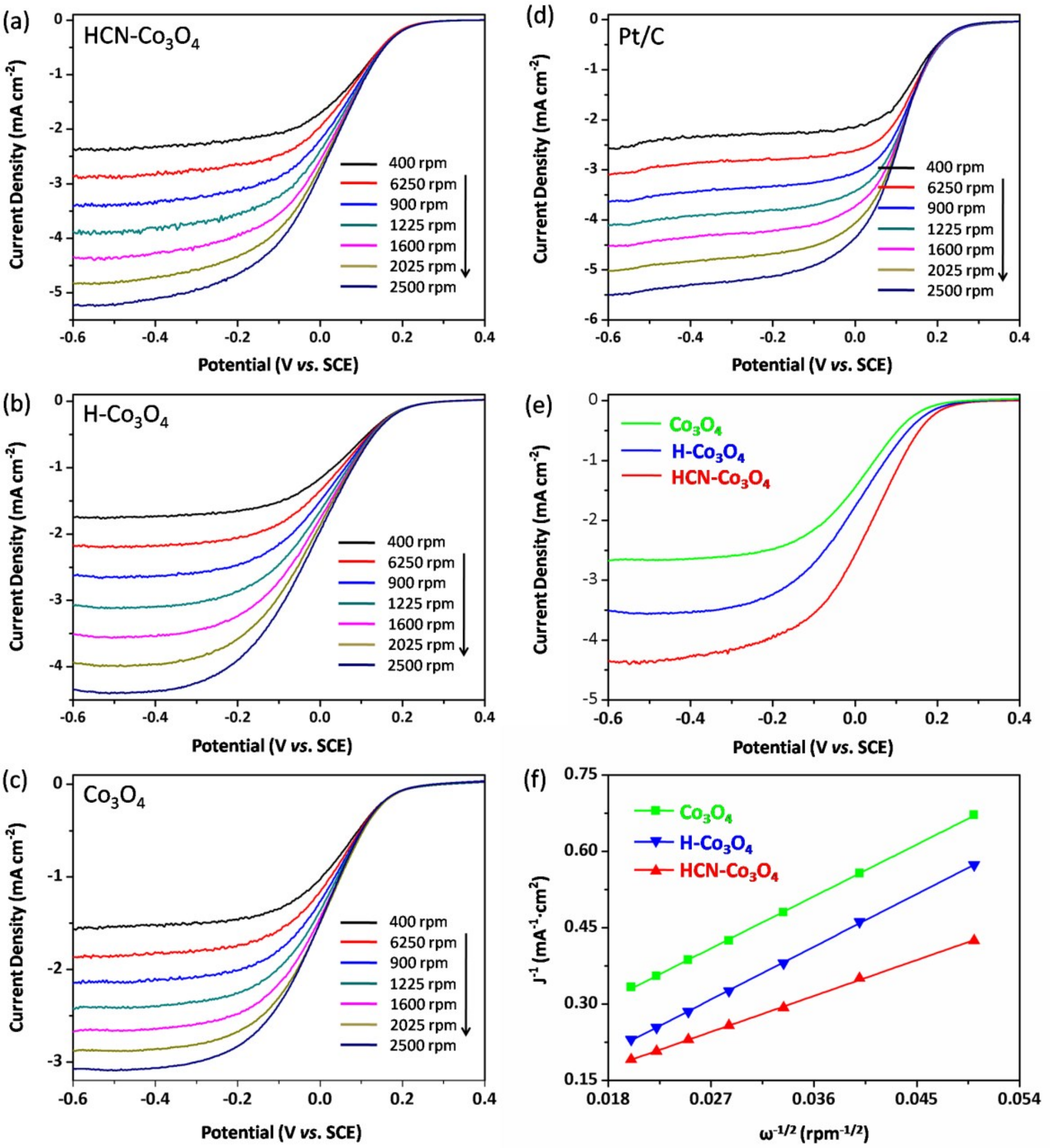

Fig. S5. (a-d) LSV curves under the different rotational speed from 400 to 2500 rpm at the 0.05 M PBS solution for different samples; (e) LSV and K-L curves of Co_3O_4, H-Co_3O_4 and HCN-Co_3O_4 obtained at 1600 rpm at the 0.05 M PBS.

Table S1. Main parameter from Nyquist curve.

Para	HCN-Co_3O_4	H-Co_3O_4	Co_3O_4
R_s (Ω)	8.07	8.37	8.61
R_{ct} (Ω)	1.02	1.98	1.24
Z_w (Ω $S^{-1/2}$)	3.19×10^{-6}	1.32×10^{-6}	9.45×10^{-5}
C (Ω^{-1} s^n cm^{-2})	8.38×10^{-6}	3.63×10^{-6}	5.93×10^{-6}
n	0.91	0.92	0.85

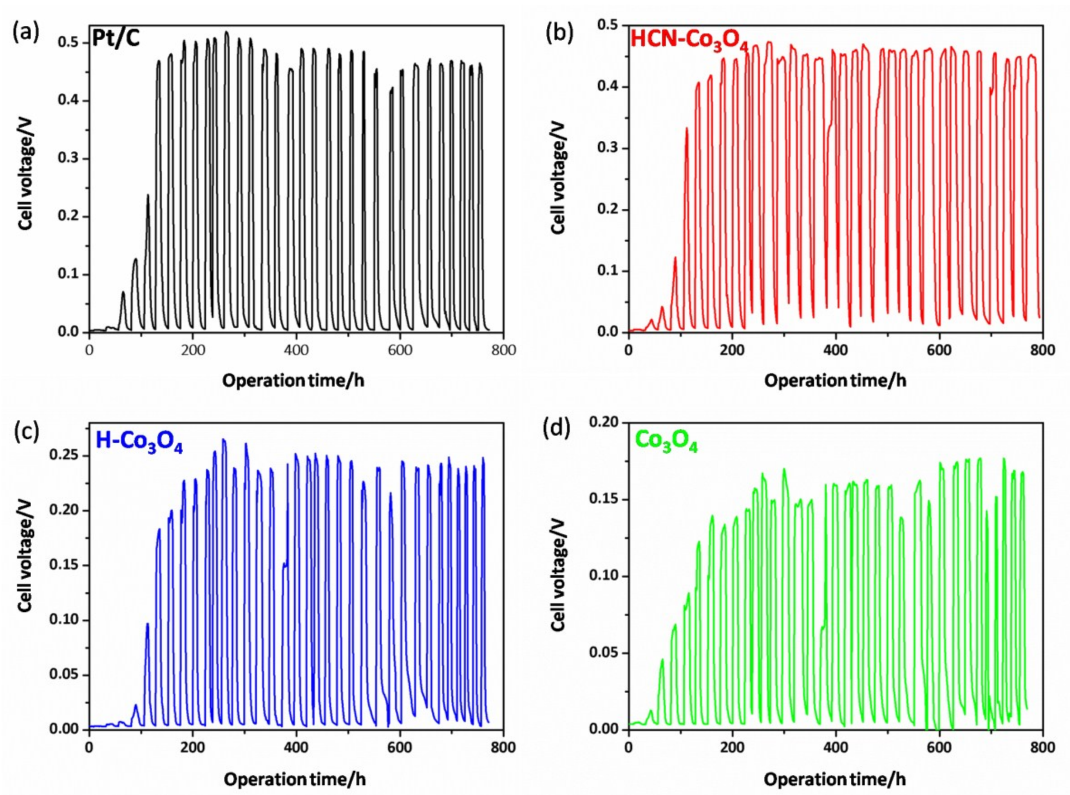

Fig. S6. (a-d) Voltage-Time profile of MFCs with different cathode catalysts.

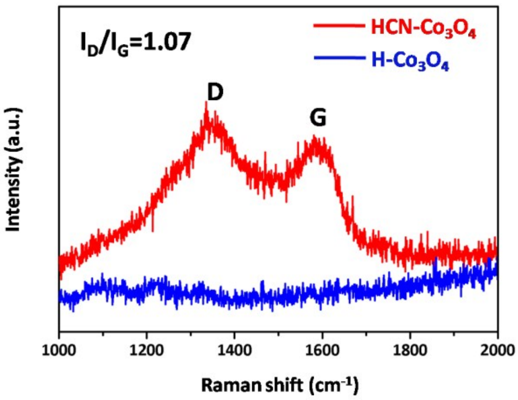

Fig. S7. Raman spectra of HCN-Co_3O_4 and H-Co_3O_4.

we have carefully characterized the HCN-Co_3O_4 and H-Co_3O_4 by Raman spectrum. The obtained spectrum have shown in Fig. S7, and the D band (1350 cm^{-1}) and G band (1580 cm^{-1}) respond to the disordered carbon and ordered carbon of the graphite carbon, respectively. There is not observable special spectra can be found in the H-Co_3O_4 composite. On the contrary, HCN-Co_3O_4 composite shows obvious D band and G hand in the Raman spectrum. The I_D/I_G value of 1.07 was illustrated that the disordered feature may be originated from the doped-nitrogen and Co_3O_4 effect. This results are in great consistent with the XRD and SEM results.

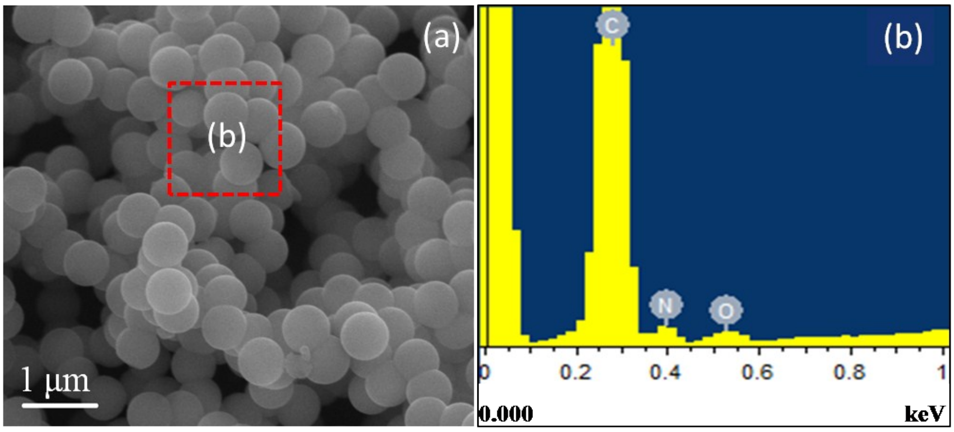

Fig. S8. (a) SEM image of the CN sphere and (b) the corresponding EDS pattern.

We have carefully characterized CN sphere by different methods. Although just a trace of N can be detected from XPS spectra of HCN-Co_3O_4 due to the coverage of dense Co_3O_4 nanoparticles on the HCN surface, the SEM image and EDS pattern of the CN sphere still indicate the substantial doping of N species into the CN sphere framework (Fig. S8).

The MFCs performance is difficult to compare directly with other literatures since the different adopted parameters, such as the organic substrate, buffer system, inoculated bacterial strain, cell configuration, catalyst content, etc. Herein, similar MFCs device were fabricated for better comparison by using commercial Pt/C as air cathode under the same identical configuration and operation conductions. The MFCs with the HCN-Co_3O_4 cathode catalyst has generated a maximum power density of 553 ± 10 mW m^{-2}, which is comparable to that of the Pt/C (535 ± 11 mW m^{-2}). Moreover, the HCN-Co_3O_4 also exhibits higher catalytic effect than that the previously reported catalysts with identical or similar mass loading. The detailed comparison was also shown in Table S**2**.

Table S2. The MFCs activity comparison with different cathodes

Reference	Mass loading [mg cm^{-2}]	Maximum power density	Maximum power density of Pt/C	Percentage to Pt/C (%)
This work	**3**	**553 ± 10 mW m^{-2}**	**535 ± 11 mW m^{-2}**	**103**
Mn-Co oxide [1]	0.5	113 ± 25 mW m^{-2}	148 ± 21 mW m^{-2}	76
CoNPc/C [2]	1.72	64.7 mW m^{-2}	81.3 mW m^{-2}	79.6
C-CoOx-FePc [3]	2.5	654 ± 32 mW m^{-2}	850 ± 42 mW m^{-2}	77.4
Co_3O_4/N-G[4]	1	1340 ± 10 mW m^{-2}	1470 ± 10 mW m^{-2}	91.1
CoTTP [5]	1	158 mW m^{-2}	171 mW m^{-2}	92.4
Bi-CoPc/C-NiO [6]	2.5	400 mW m^{-2}	450 mW m^{-2}	88.9
Porous Co_3O_4 nanorods [7]	2	503 ± 16 mW m^{-2}	-	Comparable

$(Cu_{0.3}Co_{0.7})Co_2O_4$[8]	0.5	567 mW m^{-2}	647 mW m^{-2}	87
N-G@CoNi/BCNT[9]	5	2.0 ± 0.1 W m^{-2}	2.6 ± 0.2 W m^{-2}	76.9
Urchin-like $NiCo_2O_4$/AC[10]	3	1730 ± 14 mW m^{-2}	-	Comparable

References

[1] M. Mahmoud, T. A. Gad-Allah, K. M. EI-Khatib, F. EI-Gohary, *Bioresource Technol.*, 2011, 102, 10459-10464.

[2] J. R. Kim, J.-Y. Kim, S.-B. Han, K. W. Park, G. D. Saratale, S. E. Oh, *Bioresource Technol.*, 2011, 102, 342-347.

[3] J. Ahmed, Y. Yuan, L.-H. Zhou, S. Kim, *J. Power Sources*, 2012, 208, 170-175.

[4] Y. H. Su, Y. H. Zhu, X. L. Yang, J. H. Shen, J. D. Lu, X. Y. Zhang, J. D. Chen, C. Z. Li, *Ind. Eng. Chem. Res.*, 2013, 52, 6076−6082.

[5] B. C. Liu, C. Bruckner, Y. Lei, Y. Cheng, C. Santoro, B. Li, *J. Power Sources*, 2014, 257, 246-253.

[6] B. T. Li, X. X. Zhou, X. J. Wang, B. C. Liu, B. K. Li, *J. Power Sources*, 2014, 272, 320-327.

[7] R. Kumar, L. Singh, A. W. Zularisam, F. L. Hai, *Bioresource Technol.*, 2016, 220, 537-542.

[8] V. M. Ortiz-Martinez, M. J. Salar-Garcia, K. Touati, F. J. Hernandez-Fernandez, A. P. de los Rios, F. Belhoucine, A. A. Berrabbah, *Energy*, 2016, 113, 1241-1249.

[9] Y. Hou, H. Y. Yuan, Z. H. Wen, S. M. Cui, X. R. Guo, Z. He, J. H. Chen, *J. Power Sources*, 2016, 307, 561-568.

[10] B. C. Ge, K. X. Li, Z. Fu, L. T. Pu, X. Zhang, Z. Q. Liu, K. Huang, *J. Power Sources*, 2016, 303, 325-332.